

MEGN 570: Final Project Report

Gus Floerchinger

December 17 2020

Background

Hybrid SOFC-IC Engine systems offer a unique approach to power generation due to the potential for high efficiencies ($> 70\%$) at moderate scales in the 10-100 kW range. This active area of research has traditionally been largely passed over in favor of SOFC- gas turbine (SOFC-GT) systems due to the high temperature operation of SOFC's with a Yttria-stabilized-Zirconia (YSZ) electrolyte. However, recent developments in intermediate temperature fuel cells(IT-SOFC) with a gadolinia-doped ceria (GDC) electrolyte. In addition to allowing these cells to operate at lower temperatures than traditional YSZ cells, the metal supported cells allow for operation under pressurized conditions. This can increase the cell's power density and attractiveness for use in hybrid systems. This can be seen in studies such as Seidler et al., who showed that SOFC's operating at pressure had up to a 13% increase in power density when operated at 3 bar vs atmospheric conditions.[1]

This model developed in this paper focuses specifically on the IT-SOFC developed by Leah et al. for operation in hybrid power generation systems[2], the geometry of which can be seen below.

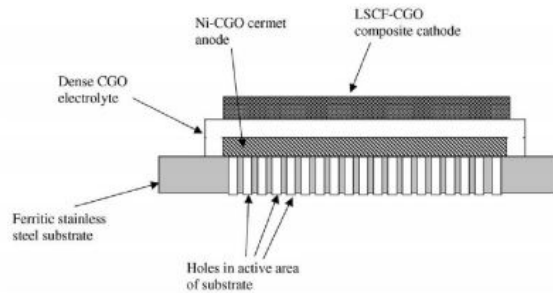


Figure 1: IT-SOFC Cell Geometry

Model Development

To Examine the effects of ASR and it's dependence on pressure, a one dimensional button cell way developed. The electrochemical reactions that the model captures are as follows:

Anode Half-Cell Reaction:



Cathode Half-Cell Reaction:



Full Cell Reaction:



Charge Transfer

changes in the cell potential due to charge transfer are characterized by the Butler-Volmer equation. This equation is to estimate kinetic losses at the electrode-electrolyte interfaces.

$$i_{far} = i_o \left[\exp\left(\frac{-\alpha_a n F \eta}{RT}\right) - \exp\left(\frac{\alpha_c n F \eta}{RT}\right) \right] \quad (4)$$

where α_a and α_c are the transfer coefficients of each reaction, η is the over-potential for the reaction, and i_o is the exchange current density, which represents the reaction rate at zero current, or at OCV conditions. for this study, the exchange current densities for the anode and cathode charge transfer reactions was estimated using equations 2 and 3 respectively[3].

$$i_{oan} = i_{oan}^{ref} \left(\frac{P_{H_2}}{P_o}\right)^{n_{H_2}} \left(\frac{P_{H_2O}}{P_o}\right)^{n_{H_2O}} \exp\left(\frac{-E_{act,an}}{R} \left(\frac{1}{T} - \frac{1}{T_{ref}}\right)\right) \quad (5)$$

$$i_{oca} = i_{oca}^{ref} \left(\frac{P_{O_2}}{P_o}\right)^{n_{O_2}} \exp\left(\frac{-E_{act,ca}}{R} \left(\frac{1}{T} - \frac{1}{T_{ref}}\right)\right) \quad (6)$$

Where i_{oan}^{ref} , n_i , and $E_{act,an}$ are empirical fitting parameters that were taken from similar performing cells as data on these parameters for CGO cells is scarce[4]. i_{oan} is a measure of the exchange current density at a reference condition with sensitivity to deviations in the partial pressure of species and temperature[5][2].

The over-potential calculated by taking the difference between the double layer potential and the half-cell potential at OCV.

$$\eta = \phi_{dl} - \phi_{OCV} \quad (7)$$

The half cell potential is a function of the species activities and the environmental conditions and is calculated by using the Nernst equation[6].

$$\phi_{OCV} = -\frac{\Delta G_{rxn}^o}{nF} - \frac{RT}{nF} \ln \left[\prod \left(\frac{P_k}{P}\right)^{\nu_k} \right] - \frac{RT}{2nF} \ln \left(\frac{P}{P_o}\right) \quad (8)$$

Because the cell cannot respond to changes in external current infinitely fast. The double layer current is introduced to enforce charge neutrality. The double layer current is a measure

of the finite progression of charge transfer reactions. It is found by taking the difference between the external current and the faradaic current.

$$i_{dl} = i_{ext} - i_{far} \quad (9)$$

This double layer current will trend to zero as the model approaches steady state at which the faradaic current will be equal to the external current.

Mass Transport

Because diffusion through the electrodes is finite, the partial pressures of species at the reaction sites will be different than in the bulk flow. To accomplish this, species transport is tracked across the electrodes using diffusion and convection mechanisms according to equation 10.

$$N_k = C_{int} X_{int} (V_{conv} + V_{difn}) \quad (10)$$

where V_{conv} and V_{difn} are the convection and diffusion velocity, respectively. The convection velocity is calculated using Darcy flow[5].

$$V_{conv} = -K_g \frac{P_2 - P_1}{\mu \Delta Y} \quad (11)$$

where K_g is the permeability of the gasses in the electrode calculated using the Kosney-Carman equation.

$$K_g = \frac{\epsilon_g^3 d_{part}^2}{72 \tau^2 (1 - \epsilon_g)^2} \quad (12)$$

The diffusion velocity is estimated using Fick's law.

$$V_{difn} = \frac{-D_k^{eff}}{X_k} \frac{X_{k,2} - X_{k,1}}{\Delta Y} \quad (13)$$

Because the pore diameter of the Ni-CGO electrode is $\approx 1 \mu m$, Knudsen diffusion as well as molecular diffusion mechanisms should be considered[7]. To capture this, an effective diffusion coefficient can be calculated by assuming that the two modes of diffusion operate in parallel as given by:

$$D_k^{eff} = \frac{\tau}{\epsilon} \left(\frac{1}{D_{kn,k}} + \frac{1}{D_{mix,k}} \right) \quad (14)$$

where $D_{kn,k}$ and $D_{mix,k}$ represent Knudsen and molecular diffusion respectively[5]. To calculate mixture averaged molecular diffusion coefficients, the binary diffusion coefficients, D_{ij} for each species are calculated using the Fuller approximation and averaged over the composition of the mixture in the electrode volume for two given species i and j[8].

$$D_{ij} = \frac{0.00143 T^{1.75}}{PM_{ij}^{0.5} [V_i^{1/3} + V_j^{1/3}]} \quad (15)$$

where P is the pressure in the electrode, V_i and V_j are the diffusion volumes for each species[8], and MM_{ij} is calculated based on the molecular weights by[3]: $MM_{ij} = 2 \left(\frac{1}{M_j} + \frac{1}{M_i} \right)^{-1}$. The binary diffusion coefficients are mixture-averaged by[3]:

$$D_{m,k} = \frac{1 - X_k}{\sum_l \frac{X_l}{D_{kl}}} \quad (16)$$

In addition to the flux of species to and from the reaction sites, the species generation, \dot{s}_k is tracked and is approximated as a function of the charge transfer using Faraday's law.

$$\dot{s}_k = \frac{i_{far} \nu_k}{nF} \quad (17)$$

where ν_k are the stoichiometric coefficients for the half cell reactions.

Governing Equations

It can be seen from equations 7 and 9 that the development of double layer current is a reaction to the transient response of the charge transfer model. This response, equal to the change in the potential difference across the double layer with time, is used as the governing differential equation for the charge transfer model and is given as:

$$\frac{\partial \Delta \phi_{dl}}{\partial t} = \frac{-i_{dl}}{C_{dl} A_{fac}} \quad (18)$$

where C_{dl} is the capacitance of the double layer, which is a measure of how quickly the double layer current decays in the presence of changes in the current. A_{fac} is the area factor representing the ratio of the cell area to the active surface area where reactions are taking place.

A balance equation for the concentration of gas phase species as a function of time is given by:

$$\frac{\partial C_k}{\partial t} = \frac{1}{\epsilon_g \Delta y} (N_{k,in} - N_{k,out} + \dot{s}_k) \quad (19)$$

where N_k is the flux of species, k across the volume boundary.

Results

The ASR was calculated using the following equation[4].

$$ASR = \frac{V_{cell} - V_{OCV}}{i_{ext}} \quad (20)$$

The ASR was solved over a range of pressures and currents to understand the effect that pressure has on the ASR. The curve of ASR vs. Pressure for three different current densities can be seen in figure 2.

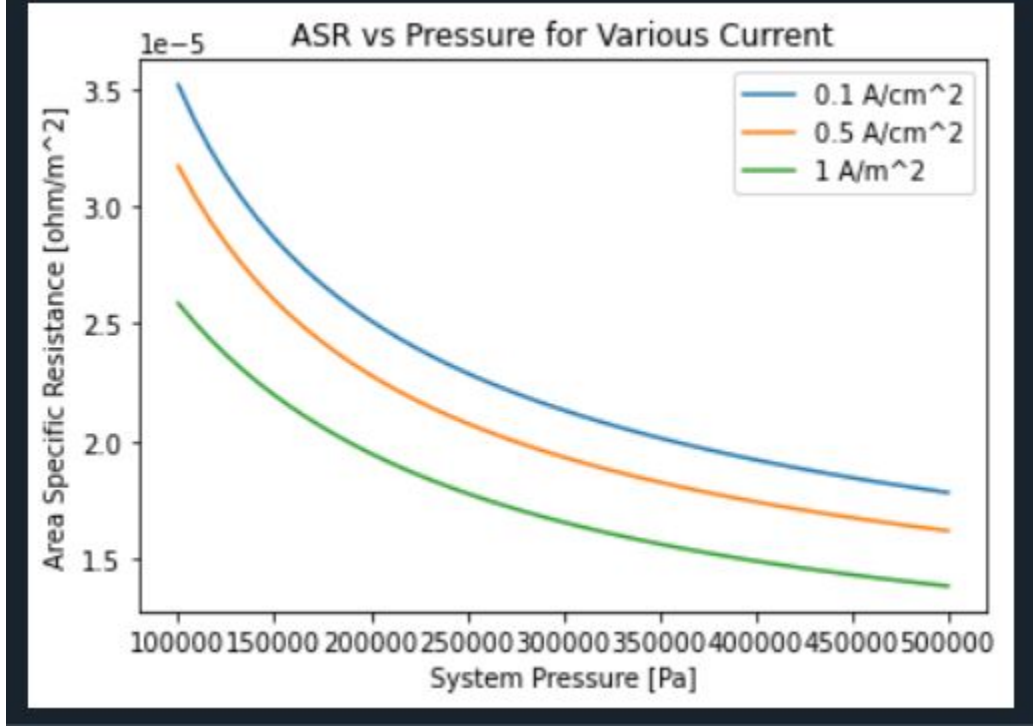


Figure 2: ASR vs. Pressure

It can be seen that both the current and pressure effect the ASR of the system. The Pressure is interesting in particular in that the effect that the pressure has tends to decay as the pressure increases. This is interesting in that it suggests that there is an optimal point at which the balance of plant BOP loads due pressuring the system will begin to outweigh the performance benefits enjoyed by reducing the ASR. The trend with pressure is most likely controlled by the pressure correction term in the OCV. This term, which shows that the OCV varies logarithmically with pressure.

. The benefits to reducing area specific resistance most directly relate to an increase in the power density of the cell. This is because the voltage that the cell is able to produce at a given current is closer to the OCV, making the cell more effective in it's operation.

Conclusion and Future Work

While the model shows a measure to able increase in performance through the ASR as a function of pressure, there are several key components that the model in its current iteration is able to capture.

The first of these is that the model neglects transport limitations in the cathode of the cell, assuming instead that the concentration of oxygen at the TPB of the cathode is approximately equal to that in the bulk flow while Leah et al. showed that this assumption is not unreasonable and that the oxygen diffusion through the cathode can be neglected, the ASR is affected by the by the change in Oxygen concentration through the OCV. This dependency should be explored in future iterations of this model.

Additionally, This model is limited in its accuracy in that it takes the entire anode as a single control volume, which was required to use some of the methods regarding mass transfer in the model. Future work should focus on making the resolution of the control volumes independent of the solution method to study the accuracy of the results, specifically because of concentration gradients that may exist within the anode, leading to non-constant rates of reaction throughout the anode and may impact the cell voltage, impacting ASR. Lastly, The model in its current state assumes that the temperature remains constant throughout operation. This is perhaps the most obvious error to the results of the study as changes in temperature can have a significant impact on the OCV. This is even more crucial for IT-SOFC's with CGO electrolytes such as the cell modeled in this study. These electrolytes can have a strong temperature dependence on properties like the conductivity and voltage leak.

References

- [1] Stephanie Seidler, Moritz Henke, Josef Kallo, Wolfgang G. Bessler, Uwe Maier, and K. Andreas Friedrich. Pressurized solid oxide fuel cells: Experimental studies and modeling. *Journal of Power Sources*, 196(17):7195–7202, September 2011.
- [2] Robert Leah, N.P. Brandon, and P. Aguiar. Modelling of Cells, Stacks and Systems Based Around Metal-Supported Planar IT-SOFC Cells with CGO Electrolytes Operating at 500–600°C. *Journal of Power Sources*, 145:336–352, August 2005.
- [3] P. Kazempoor, V. Dorer, and F. Ommi. Modelling and Performance Evaluation of Solid Oxide Fuel Cell for Building Integrated Co- and Polygeneration. *Fuel Cells*, 10(6):1074–1094, 2010. eprint: <https://onlinelibrary.wiley.com/doi/pdf/10.1002/fuce.200900082>.
- [4] Christopher H Wendel. *DESIGN AND ANALYSIS OF REVERSIBLE SOLID OXIDE CELL SYSTEMS FOR ELECTRICAL ENERGY STORAGE*. PhD thesis, 2015.
- [5] S. Campanari and P. Iora. Definition and sensitivity analysis of a finite volume SOFC model for a tubular cell geometry. *Journal of Power Sources*, 132(1):113–126, May 2004.
- [6] P. Kazempoor and R. J. Braun. Model validation and performance analysis of regenerative solid oxide cells for energy storage applications: Reversible operation. *International Journal of Hydrogen Energy*, 39(11):5955–5971, April 2014.
- [7] Daniel A. Macedo, Filipe M. L. Figueiredo, Carlos A. Paskocimas, Antonio E. Martinelli, Rubens M. Nascimento, and Fernando M. B. Marques. Ni-CGO cermet anodes from nanocomposite powders: Microstructural and electrochemical assessment. *Ceramics International*, 40(8, Part B):13105–13113, September 2014.
- [8] The Properties of Gases and Liquids, 5th Edition By Bruce E. Poling (University of Toledo), John M. Prausnitz (University of California at Berkeley), and John P. O’Connell (University of Virginia). McGraw-Hill: New York. 2001. 768 pp. \$115.00. ISBN 0-07-011682-2. | Journal of the American Chemical Society.